BOREAL ENVIRONMENT RESEARCH 21: 274–286
ISSN 1239-6095 (print) ISSN 1797-2469 (online)

Helsinki 23 May 2016

Intermediate ions as a strong indicator of new particle formation bursts in a boreal forest

Katri Leino[1,*], Tuomo Nieminen[1,2], Hanna E. Manninen[1], Tuukka Petäjä[1], Veli-Matti Kerminen[1] and Markku Kulmala[1]

[1)] *Department of Physics, P.O. Box 64, FI-00014 University of Helsinki, Finland (*corresponding author's email: katri.e.leino@helsinki.fi)*
[2)] *University of Eastern Finland, Department of Applied Physics, P.O. Box 1627, FI-70211 Kuopio, Finland*

Received 12 Nov. 2015, final version received 22 Feb. 2016, accepted 1 Mar. 2016

Leino K., Nieminen T., Manninen H.E., Petäjä T., Kerminen V.-M. & Kulmala M. 2016: Intermediate ions as a strong indicator for new particle formation bursts in a boreal forest. *Boreal Env. Res.* 21: 274–286.

Secondary aerosol formation from gas-phase precursors is a frequent phenomenon occurring in a boreal environment. Traditionally, this process is identified visually from observational data on total and ion number size distributions. Here, we introduce a new, objective classification method for the new particle formation events based on measured intermediate-ion concentrations. The intermediate-ion concentration is a suitable indicator of new particle formation, because it is linked to the atmospheric new particle formation. The concentration of intermediate ions is typically very low (below 5 cm^{-3}) when there is no new particle formation or precipitation events occurring. In this study, we analysed concentrations of negative intermediate ions at the Station for Measuring Ecosystem Atmosphere Relations (SMEAR II) in Hyytiälä, Finland, during the years 2003–2013. We found that the half-hour median concentration of negative intermediate ions in sizes 2–4 nm was > 20 cm^{-3} during 77.5% of event days classified by traditional method. The corresponding value was 92.3% in the case of 2–7 nm negative ions. In addition, the intermediate-ion concentration varied seasonally in a similar manner as the number of event days, peaking in the spring. A typical diurnal variation of the intermediate-ion concentration resembled that of the particle concentration during the event days. We developed here a new method for classifying new particle formation events based on intermediate-ion concentrations. The new method is complementary to the traditional event analysis and it can also be used as an automatic way of determining new particle formation events from large data sets.

Introduction

Atmospheric aerosol particles affect the Earth's climate by scattering and absorbing solar radiation and by affecting cloud properties (e.g. Myhre 2009, IPCC 2013). A major source of aerosol particles in terms of their number concentrations is atmospheric new particle formation (NPF), which can be divided into neutral and ion-induced or ion-mediated pathways (Curtius *et al*. 2006, Kulmala *et al*. 2007, Hirsikko *et al*. 2011, Iida *et al*. 2006, Yu and Turco 2008). Our understanding of atmospheric NPF is far from perfect, and analysing long-term observational data sets is one very important way to improve it (Kulmala *et al*. 2004, 2013, Nieminen *et al*.

Editor in charge of this article: Hannele Korhonen

2014). In this respect, it is essential to identify reliably, yet relatively easily, when NPF is taking place in the atmosphere.

Several studies on small aerosol particles and ions down to sizes of about 1 nm in diameter were carried out (e.g. Jiang *et al*. 2011, Kuang *et al*. 2012, Kulmala *et al*. 2013). Kulmala *et al*. (2013) suggested 2 nm as a critical size for detecting atmospheric NPF events because of the following reasons: (1) the growth < 1.3 nm diameter (Millikan) clusters is usually very slow, so this size range has probably no direct connection to atmospheric NPF; (2) while 1.3–1.5 nm clusters start to be stabilized by amines, ammonia and organic vapours, their formation may not lead to a NPF event; and (3) activation of growing clusters seems to begin between 1.5 and 2 nm after which the clusters grow relatively fast, especially during active formation events (Kulmala *et al*. 2013).

In addition to the neutral aerosol particles, small ions defined as charged particles < 1.6 nm in diameter exist almost all the time in the atmosphere (Hirsikko *et al*. 2011). The small ions are formed mainly via the ionisation of air molecules by radon decay, gamma radiation and cosmic radiation (Israël 1970, Flagan 1998, Laakso *et al*. 2004). The number concentration of the small ions varies. Typical concentrations of positive and negative small ions are in the range of 200–2500 cm^{-3} and their atmospheric lifetimes are very short (Vana *et al*. 2007, Komppula *et al*. 2007, Hirsikko *et al*. 2005). The electrode effect may lead to observing slightly more positive small ions when sampled close to the ground level (Hoppel, 1967). This explains why the concentration of positive small ions is normally higher than negative cluster ions at Hyytiälä. Above the small-/cluster-ion mode, the number concentration of positive and negative ions should show similar concentrations, since atmospheric ions are expected to be in a charge equilibrium in most environments. Intermediate ions are somewhat larger than small ions, having diameters (Millikan) in the range of 2.0–7.8 nm (0.034–0.5 $cm^2\ V^{-1}\ s^{-1}$ in ion mobility; Hõrrak *et al*. 2000). Intermediate ions are formed by the growth of small ions, originating possibly from an ion-induced formation pathway, or by small ions attaching on particles formed via neutral particle formation mechanisms. In addition to NPF, other possible sources for small and intermediate ions are rainfall (Tammet *et al*. 2009, Kolarž *et al*. 2012), heavy snowfall (Virkkula *et al*. 2007), thunderstorms (D'Alessandro *et al*. 2009), powerlines (Jayaratne *et al*. 2008) and vehicle emissions (Gopalakrishnan *et al*. 2005, Jayaratne *et al*. 2010).

Atmospheric NPF and intermediate-ion number concentration are expected to be linked to each other, since a fraction of newly-formed particles will acquire an electric charge during a NPF event (e.g. Gagné *et al*. 2010). This, together with the high sensitivity of ion spectrometers in detecting small increases in intermediate-ion concentrations during the very first steps of NPF (Hirsikko *et al*. 2007, Asmi *et al*. 2009) indicates that NPF could be identified based on an enhanced intermediate-ion concentration.

The occurrence of NPF has usually been estimated visually from measured particle number size distribution plots following the methods introduced by Dal Maso *et al*. (2005). In those methods, each day of the measurement data set is classified as event, non-event or undefined according to the criteria explained in more detail by Dal Maso *et al*. (2005) and Hirsikko *et al*. (2007). This visual classification method is slow and subjective. Therefore, in this work we introduce the use of intermediate-ion concentrations as a method for identifying NPF events in a boreal forest environment. We used the ion number size distribution and total particle concentration measurements from Hyytiälä, Finland, collected during 2003–2013, to study the validity of this method. Data for periods with precipitation were ignored and the rain-induced intermediate-ion formation and snowfall-related intermediate ions were not considered. The specific aim of this work was to find out how well the occurrence of NPF events can be defined using intermediate-ion number concentrations, particularly in size ranges of 2–4 nm and 2–7 nm.

Material and methods

We utilized long-term observational data from the Station for Measuring Forest Ecosystem–Atmosphere Relations (SMEAR II) located in a boreal forest in Hyytiälä (southern Finland

61°51´N, 24°17´E, 181 a.s.l.; *see* Hari and Kulmala 2005). The station is equipped with several instruments performing aerosol and gas measurements, and comprehensive data sets have been collected continuously since 1996 (Kulmala *et al*. 2001). Measurements of the mobility distributions of charged aerosol particles and clusters in the size range of 0.8–47 nm with an Air Ion Spectrometer (AIS, Airel Ltd., Estonia) commenced in August 2003, and since 2006 they have been carried out with its modified version: Neutral cluster and Air Ion Spectrometer (NAIS, Airel Ltd., Estonia). The operation principles of the AIS and NAIS are presented in Mirme *et al*. (2007 and 2013, respectively), and Hirsikko *et al*. (2005) reports the first AIS results from the SMEAR II station. Kulmala *et al*. (2007) and Manninen *et al*. (2009) report the first long-term measurements using NAIS at Hyytiälä. The number size distributions of aerosol particles have been measured with a Differential Mobility Particle Sizer (DMPS) since 1996; the instrument is described in detail by Aalto *et al*. (2001). The locations of all instruments have been the same since 2004.

To identify rain episodes, we used the precipitation intensity data measured with a FD12P weather sensor (Vaisala Oyj, Helsinki, Finland) above the forest at the 18-m height. FD12P measures all precipitation as liquid water, and converts the portion of snow to snowfall. The precipitation measurements are made at the 1-min intervals. The precipitation intensity data are given as medians over a 30-min averaging period, while the precipitation and snowfall data are given as accumulated values for a 30-min averaging period.

Ion and particle number size distribution measurements

AIS (Mirme *et al*. 2007) is a multichannel, and BSMA (Tammet 2006) is a single-channel spectrometer which measure naturally-charged air ions. NAIS (Mirme and Mirme 2013) is a modified version of AIS, and in addition to naturally charged ions, it also measures neutral aerosol particles and clusters with a controlled charging of an aerosol sample. (N)AIS classifies ions according to their electrical mobility (Manninen *et al*. 2009). The instrument consists of two parallel differential mobility analysers (DMA), one for positive ions and the other for negative ions. Both DMAs are divided into 21 insulated collector electrodes and the collected ions are measured simultaneously. AIS and NAIS operate at a 30-liter per minute (LPM) sample flow and 60 LPM sheath air flow per analyser. The mobility range of AIS is 3.16–0.001 $cm^2\ V^{-1}\ s^{-1}$, which corresponds to a mobility diameter range of 0.8–47 nm (Millikan-Fuchs equivalent diameter; Mäkelä *et al*. 1996). The ion mobility distributions were measured in 5-min cycles with NAIS and in 10-min cycles with BSMA. For the same instrument type, the measured concentration can differ among the instruments by up to 10% (Gagné *et al*. 2011). Both, AIS and NAIS were used in several inter-comparison experiments in laboratory conditions (Asmi *et al*. 2009, Gagné *et al*. 2011, Wagner *et al*. 2016). According to Wagner *et al*. (2016), the number concentrations measured by NAIS are underestimated by 15%–30%, especially at the lower end of the measurement size range (below 10 nm). However, the sizing information (mode diameter determined from number size distributions measured by the NAIS) is very accurate. Especially in the size range 2–4 nm, the particle diameter measured by NAIS matches the diameter selected by the reference DMA within 1%. The size and concentration resolutions of NAIS depend on the signal to noise ratio (Mirme and Mirme 2013). DMPS determined the aerosol number size distribution in the diameter size ranges of 3–1000 nm with 10-min resolution. Before the classification of an aerosol population, the particles are transported to a radioactive source where they reach a constant bipolar charge equilibrium. DMPS contains two parallel DMAs and the particle number concentrations are determined with two Condensation Particle Counters (CPC) with different cut-offs. A detailed description of the instrument is presented in Aalto *et al*. (2001). DMPS has a resolution of

$$R = \frac{Z^*}{\Delta Z_{1/2}} = 5, \quad (1)$$

which is the ratio of the mobility corresponding to the peak in the transfer function, Z^*, to the full

width of the transfer function at one-half of the maximum value, $\Delta Z_{1/2}$ (Flagan 1998). Using an electrometer as a detector in DMPS, the accuracy of the concentration measurement is ±10%.

Identifying NPF events from measured ion number size distributions

The analysis was performed by classifying each day of the period 2003–2013 either as an event or non-event day based on the maximum ion concentration during that day. In the first step, we calculated the half-hour median concentration of naturally-charged intermediate air ions (negative and positive ions, separately) in different size ranges (2–3 nm, 2–4 nm, 2–5 nm, 2–6 nm, 2–7 nm and 3–7 nm). In the next step, two size ranges (2–4 nm and 2–7 nm) and negative polarity were selected for a closer investigation. It is certain that the size range of 2–4 nm includes newly-formed intermediate ions. We classified the days according to whether the maximum 2–4 nm ion concentration reached > 100 cm^{-3}, > 50 cm^{-3}, > 40 cm^{-3}, > 30 cm^{-3} or > 20 cm^{-3} during the day, and whether the maximum of 2–7 nm ion concentration reached > 100 cm^{-3}, > 80 cm^{-3}, > 70 cm^{-3}, > 60 cm^{-3}, > 50 cm^{-3}, > 30 cm^{-3} or > 20 cm^{-3} during the same day. In the third step, we further classified the days according to whether the ion concentration persisted above the concentration limits given above for at least 1 hour or 2 hours. All these criteria were tested to find out how well they perform in differentiating between the NPF event and non-event days. The data from periods with precipitation were not included in the analysis.

We compared our event-day classification with the traditional visual event classification based on the Differential Mobility Particle Sizer (DMPS) measurements carried out at the same location, according to which each day was classified either as a particle formation event, undefined or non-event day based on size range concentrations (Dal Maso *et al*. 2005, Hirsikko *et al*. 2007).

In addition to finding out whether our classification method is capable of separating between NPF event and non-event, we were interested in two types of borderline cases: (1) the days when the intermediate-ion concentration was elevated, but the growth of newly formed particles had been stalled before the lower size limit of DMPS measurements (Hirsikko *et al*. 2007); and (2) the DMPS-based NPF event days, during which the intermediate-ion concentration was below the typical values (< 20 cm^{-3}) associated with NPF events. The latter could be due to the onset of NPF taking place in some other part of the atmosphere than the surface layer where the aerosol measurements for this study were made.

Results and discussion

General characteristics of NPF and intermediate-ion concentrations

A typical NPF event in Hyytiälä starts before noon and growth of the particles continues for several hours (Mäkelä *et al*. 1997, Mäkelä *et al*. 2000, Aalto *et al*. 2001). We selected one day as an example to illustrate how NPF is seen in particle number size distribution measurements (Fig. 1). On this day, a homogeneously continuing and distinct particle formation and growth that started at about 09:00 local time was observed. The particle formation began at the sub-3 nm range, in other words, small ions and molecular clusters were activated in the morning and started to grow in sizes. After about 18:00, a second increase in the concentrations of ions up to 3 nm in diameter was observed (Figs. 1 and 2). This type of a cluster ion event occurs frequently in Hyytiälä during the nights preceding or following a NPF event (Junninen *et al*. 2008, Buenrostro Mazon *et al*. 2016). Such events do not lead to the formation and growth of ions larger than approx. 3 nm in diameter. In order to exclude such cases from our study, we considered only the data measured between 06:00 and 18:00.

When plotting the time series of the intermediate ions, the NPF burst was clearly visible as a sudden increase in the 2–7 nm ion concentration (Fig. 2). We calculated half-hour median concentrations of ions from the measurement data and ignored all periods with precipitation, both in a form of snow and liquid. The half-hour median concentration seemed to be a good approximation for the 5-min resolution original data

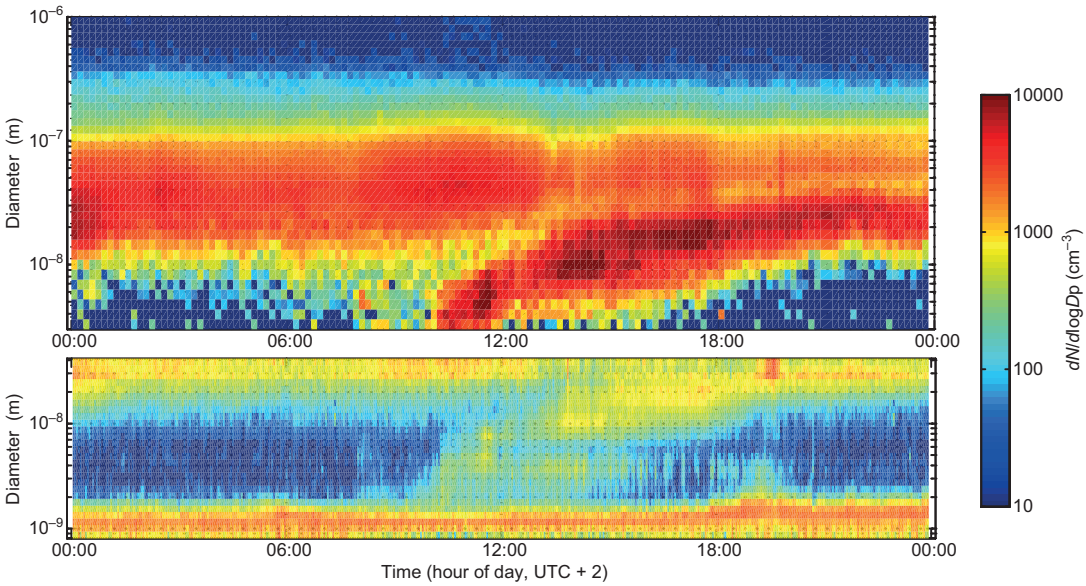

Fig. 1. Total particle size distribution measured with DMPS (top) and negative air ion size distribution measured with NAIS ion mode (bottom) during a typical NPF event day (4 Apr. 2013) at the SMEAR II station in Hyytiälä.

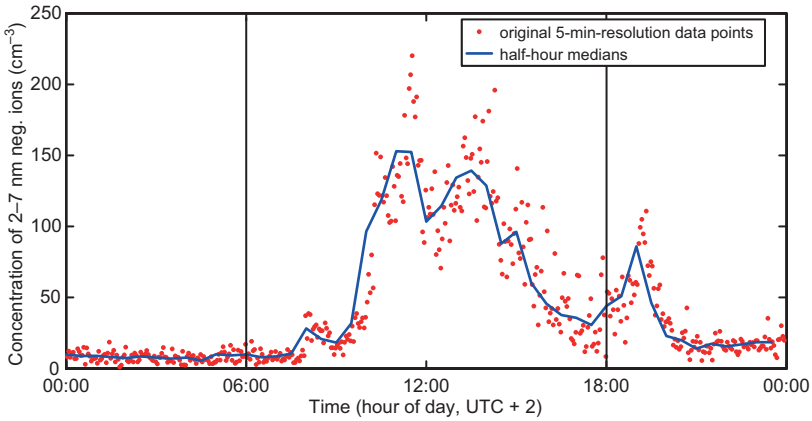

Fig. 2. Differences between 5-min-resolution original data points (red dots) and calculated half-hour median concentrations of negative intermediate ions in size range of 2–7 nm (blue line) on 4 Apr. 2013 at the SMEAR II station, Hyytiälä.

(Fig. 2), so in the further analysis we used the 30-min median values. In later analysis, we used the daily maximum concentration of intermediate ions to identify the NPF event burst. According to this study and earlier results (e.g. Laakso *et al*. 2007, Hirsikko *et al*. 2007, 2011), higher than typical concentrations of negative intermediate ions are detected in Hyytiälä. We therefore focused our analysis on negative ion concentrations, even though also positive ion concentrations could have been used in this method.

The ion data from Hyytiälä obtained with AIS covered 74% of the days between the years of 2003 and 2013. Intermediate-ion concentrations in the size ranges of 2–4 nm and 2–7 nm (Fig. 3) varied roughly (5–95 percentiles) in the ranges 0.5–30 cm^{-3} and 1.5–60 cm^{-3}, respectively. The corresponding ranges for positive ions were 0.6–20 cm^{-3} and 1.6–50 cm^{-3}. The most common intermediate-negative-ion concentration ranges were 1–10 cm^{-3} for 2–4 nm ions and 2–20 cm^{-3} for 2–7 nm ions (Fig. 3). The ion concentration distributions differed little between the daytime and all data (Fig. 3).

Monthly-mean concentrations of the intermediate ions at our measurement site have been

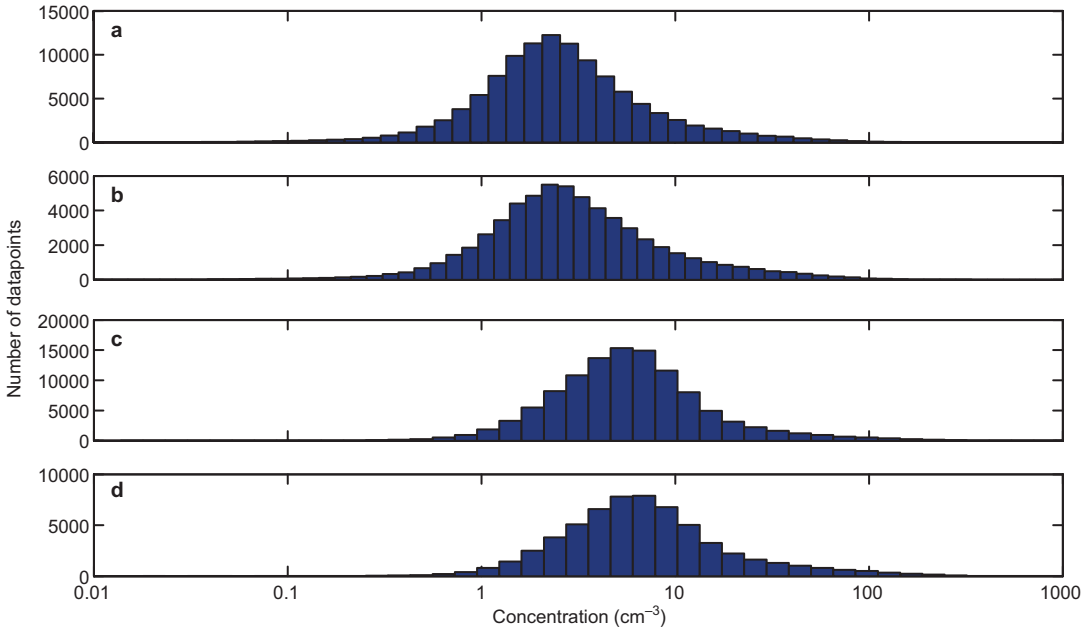

Fig. 3. Histograms of the variation of the half-hour median concentrations of (**a**) 2–4 nm negative ions (all data), (**b**) 2–4 nm negative ions (daytime [06:00–18:00] data), (**c**) 2–7 nm negative ions (all data), and (**d**) 2–7 nm negative ions (daytime [06:00–18:00] data) at the SMEAR II station in 2003–2013.

reported to be in the range < 1–25 cm^{-3} for both polarities, being somewhat higher for the negative than positive ions (Hirsikko *et al*. 2005). For comparison, the annual-average concentration of intermediate ions (1.5–7.5 nm in diameter) in Tartu, Estonia, was found to be about 40 cm^{-3} with 5% of the measurements having concentrations < 10 cm^{-3} (Tammet *et al*. 2014).

Identifying NPF events using intermediate ions

The intermediate-negative-ion concentration in both size ranges (2–4 nm and 2–7 nm) differed clearly among the NPF event, non-event and undefined days, as classified by the DMPS-based event analysis (Figs. 4 and 5). This result indicates that the intermediate-ion concentration serves as a good proxy for the occurrence of NPF in all seasons. The background concentration of intermediate ions was typically below 5 cm^{-3} when no NPF was taking place, or if a precipitation event occurred.

The comparison between DMPS-based and intermediate ion-based event analysis was performed for daytime (06:00–18:00) intermediate-ion concentrations. On 23% of the DMPS-based event days, we did not detect elevated (at least 20 ions in cm^{-3}) intermediate-negative-ion concentrations in the size range of 2–4 nm during the daytime (Table 1). The corresponding fraction of days was about 8% for negative intermediate ions in the size range of 2–7 nm (Table 2). These findings can be explained by the fact that the charging probability of ions in this size range is only about 1%–3% (Wiedensohler 1988), and that neutral NPF was probably dominating on those days, which seems to be a common situation in Hyytiälä (Gagne *et al*. 2010). On 2%–16% of the DMPS-based non-events days, the maximum concentration of 2–4 nm negative ions exceeded some of the chosen ion concentration thresholds (Table 1). The corresponding fraction of days was 4%–31% for negative intermediate ions in the size range of 2–7 nm (Table 2). One explanation for this finding is that newly formed clusters and intermediate ions do not always grow into the larger sizes, so that these days are not defined as NPF events in the DMPS-based event classification.

By requiring that the intermediate-ion concentration remains elevated (above the thresh-

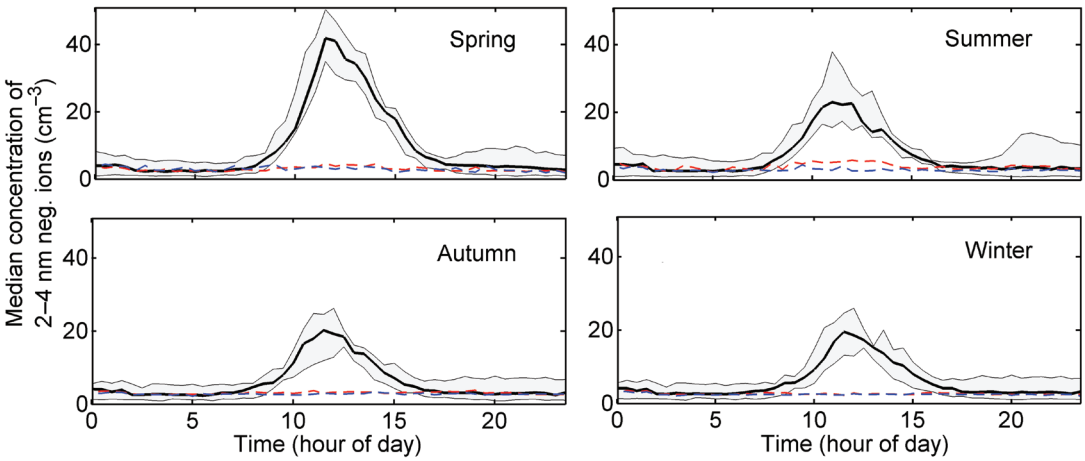

Fig. 4. Diurnal variations of the median 2–4 nm negative ion concentration during the NPF event, non-event and undefined days in different seasons in the years of 2003–2013. The thick black line indicates median concentrations during event days, grey areas are 25%–75% percentiles, the dashed blue line indicates median concentrations during non-event days, and the dashed red line indicates undefined days. The event day classification was determined by ordinary NPF event analysis based on DMPS size distributions.

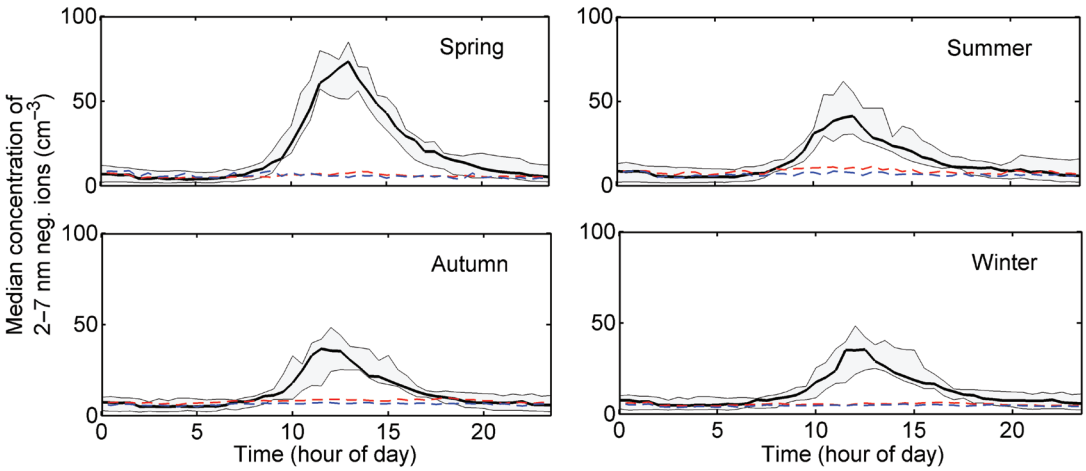

Fig. 5. Same as Fig. 4 but for 2–7 nm negative ion concentrations.

old value) continuously for 1 hour or 2 hours, somewhat smaller fraction (49%–63% in case of 2–4 nm negative ions) of the event days classified by DMPS-based event classification was identified when using our new method. At the same time, however, a considerably smaller fraction (2%–4% in case of 2–4 nm negative ions) of the DMPS-based non-event days became classified as potential NPF events.

According to the DMPS-based event classification, 77%, 12% and 11% of the days when the negative 2–4 nm ion concentration exceeded 100 cm^{-3} during daytime were classified as NPF event, undefined and non-event days, respectively (Table 3). Relatively similar results were obtained for the negative 2–7 nm ion concentration (Table 4). To eliminate miss-leading results concerning NPF events, we took into account cases of elevated concentrations persisting for at least 1 h or 2 h only. As a result, only 1.3% or 0.6% of the days when negative ions were continuously over 100 cm^{-3} for at least 1 h or 2 h, respectively, had been classified as non-event days based on the DMPS data. This indicates

Table 1. Numbers and respective percentages (in parentheses) of event, undefined and non-event days in 2003–2013, during which the concentration of 2–4 nm negative ions exceed a given concentration threshold: in the case '0 h', it is enough that the maximum ion concentration exceeds the concentration threshold, whereas in the cases '1 h' and '2 h', the ion concentrations need to remain above the threshold value for at least 1 and 2 hours, respectively. Only daytime (06:00–18:00) data were taken into account. Total numbers (100%) of DMPS-based event, undefined and non-event days used to calculate percentages are given in in the first column in parentheses.

	Concentration threshold (cm^{-3})	0 h	1 h	2 h
Event days (702)	100	122 (17.4)	44 (6.3)	13 (1.9)
	50	334 (47.6)	192 (27.4)	125 (17.8)
	40	394 (56.1)	252 (35.9)	166 (23.6)
	30	468 (66.7)	332 (47.3)	239 (34.0)
	20	544 (77.5)	439 (62.5)	341 (48.6)
Undefined days (1090)	100	19 (1.7)	4 (0.4)	1 (0.1)
	50	71 (6.5)	16 (1.5)	9 (0.8)
	40	108 (9.9)	26 (2.4)	14 (1.3)
	30	178 (16.3)	49 (4.5)	21 (1.9)
	20	303 (27.8)	107 (9.8)	46 (4.2)
Non-event days (976)	100	17 (1.7)	2 (0.2)	1 (0.1)
	50	42 (4.3)	7 (0.7)	4 (0.4)
	40	60 (6.1)	13 (1.3)	4 (0.4)
	30	88 (9.0)	24 (2.5)	8 (0.8)
	20	154 (15.8)	41 (4.2)	22 (2.3)

Table 2. Numbers and respective percentages (in parentheses) of event, undefined and non-event days in 2003–2013, during which the concentration of 2–7 nm negative ions exceed a given concentration threshold: in the case '0 h', it is enough that the maximum ion concentration exceeds the concentration threshold, whereas in the cases '1 h' and '2 h', the ion concentrations need to remain above the threshold value for at least 1 and 2 hours, respectively. Only daytime (06:00–18:00) data were taken into account. Total numbers (100%) of DMPS-based event, undefined and non-event days used to calculate percentages are given in the first column in parentheses.

	Concentration (cm^{-3}) threshold (cm^{-3})	0 h	1 h	2 h
Event days (702)	100	309 (44.0)	174 (24.8)	117 (16.7)
	80	381 (54.3)	246 (35.0)	155 (22.1)
	70	404 (57.5)	286 (40.7)	189 (26.9)
	60	437 (62.3)	327 (46.6)	221 (31.5)
	50	475 (67.7)	360 (51.3)	273 (38.9)
	30	591 (84.2)	469 (66.8)	380 (54.1)
	20	648 (92.3)	572 (81.5)	501 (71.4)
Undefined days (1090)	100	75 (6.9)	15 (1.4)	5 (0.5)
	80	101 (9.3)	23 (2.1)	11 (1.0)
	70	119 (10.9)	30 (2.8)	15 (1.4)
	60	150 (13.8)	42 (3.9)	19 (1.7)
	50	192 (17.6)	51 (4.7)	23 (2.1)
	30	358 (32.8)	130 (11.9)	55 (5.0)
	20	556 (51.0)	275 (25.2)	148 (13.6)
Non-event days (976)	100	43 (4.4)	8 (0.8)	2 (0.2)
	80	52 (5.3)	12 (1.2)	4 (0.4)
	70	60 (6.1)	17 (1.7)	5 (0.5)
	60	72 (7.4)	22 (2.3)	8 (0.8)
	50	93 (9.5)	28 (2.9)	12 (1.2)
	30	185 (19.0)	54 (5.5)	27 (2.8)
	20	302 (30.9)	106 (10.9)	68 (7.0)

Table 3. Numbers of days when 2–4 nm negative ions exceeded a given concentration threshold, and the distribution of these days among the DMPS-based event, undefined and non-event days in 2003–2013. In the case '0 h', it is enough that the maximum ion concentration exceeds the concentration threshold, whereas in the cases '1 h' and '2 h', the ion concentrations need to remain above the threshold value for at least 1 and 2 hours, respectively. The value in parentheses is the percentage of the days of the total number of days on which the corresponding concentration threshold was exceeded. Only daytime (06:00–18:00) ion data were taken into account.

	Concentration threshold (cm^{-3})	Total number of ion-method-based event days	0 h	1 h	2 h
Event days	100	158	122 (77.2)	44 (27.8)	13 (8.2)
	50	447	334 (74.7)	192 (43.0)	125 (28.0)
	40	562	394 (70.1)	252 (44.8)	166 (29.5)
	30	734	468 (63.8)	332 (45.2)	239 (32.6)
	20	1001	544 (54.3)	439 (43.9)	341 (34.1)
Undefined days	100	158	19 (12.0)	4 (2.5)	1 (0.6)
	50	447	71 (15.9)	16 (3.6)	9 (2.0)
	40	562	108 (19.2)	26 (4.6)	14 (2.5)
	30	734	178 (24.3)	49 (6.7)	21 (2.9)
	20	1001	303 (30.3)	107 (10.7)	46 (4.6)
Non-event days	100	158	17 (10.8)	2 (1.3)	1 (0.6)
	50	447	42 (9.4)	7 (1.6)	4 (0.9)
	40	562	60 (10.7)	13 (2.3)	4 (0.7)
	30	734	88 (12.0)	24 (3.3)	8 (1.1)
	20	1001	154 (15.4)	41 (4.1)	22 (2.2)

Table 4. Numbers of days when 2–7 nm negative ions exceeded a given concentration threshold, and the distribution of these days among the DMPS-based event, undefined and non-event days in 2003–2013. In the case '0 h', it is enough that the maximum ion concentration exceeds the concentration threshold, whereas in the cases '1 h' and '2 h', the ion concentrations need to remain above the threshold value for at least 1 and 2 hours, respectively. The value in parentheses is the percentage of the days of the total number of days on which the corresponding concentration threshold was exceeded. Only daytime (06:00–18:00) ion data were taken into account.

	Concentration threshold (cm^{-3})	Total number of ion-method-based event days	0 h	1 h	2 h
Event days	100	427	309 (72.4)	174 (40.7)	117 (27.4)
	80	534	381 (71.3)	246 (46.1)	155 (29.0)
	70	583	404 (69.3)	286 (49.1)	189 (32.4)
	60	659	437 (66.3)	327 (49.6)	221 (33.5)
	50	760	475 (62.5)	360 (47.4)	273 (35.9)
	30	1134	591 (52.1)	469 (41.4)	380 (33.5)
	20	1506	648 (43.0)	572 (38.0)	501 (33.3)
Undefined days	100	427	75 (17.6)	15 (3.5)	5 (1.2)
	80	534	101 (18.9)	23 (4.3)	11 (2.1)
	70	583	119 (20.4)	30 (5.1)	15 (2.3)
	60	659	150 (22.8)	42 (6.4)	19 (2.9)
	50	760	192 (25.3)	51 (6.7)	23 (3.0)
	30	1134	358 (31.6)	130 (11.5)	55 (4.9)
	20	1506	556 (36.9)	275 (18.3)	148 (9.8)
Non-event days	100	427	43 (10.1)	8 (1.9)	2 (0.5)
	80	534	52 (9.7)	12 (2.2)	4 (0.8)
	70	583	60 (10.3)	17 (2.9)	5 (0.9)
	60	659	72 (10.9)	22 (3.3)	8 (1.2)
	50	760	93 (12.2)	28 (3.7)	12 (1.6)
	30	1134	185 (16.3)	54 (4.8)	27 (2.4)
	20	1506	302 (20.1)	106 (7.0)	68 (4.5)

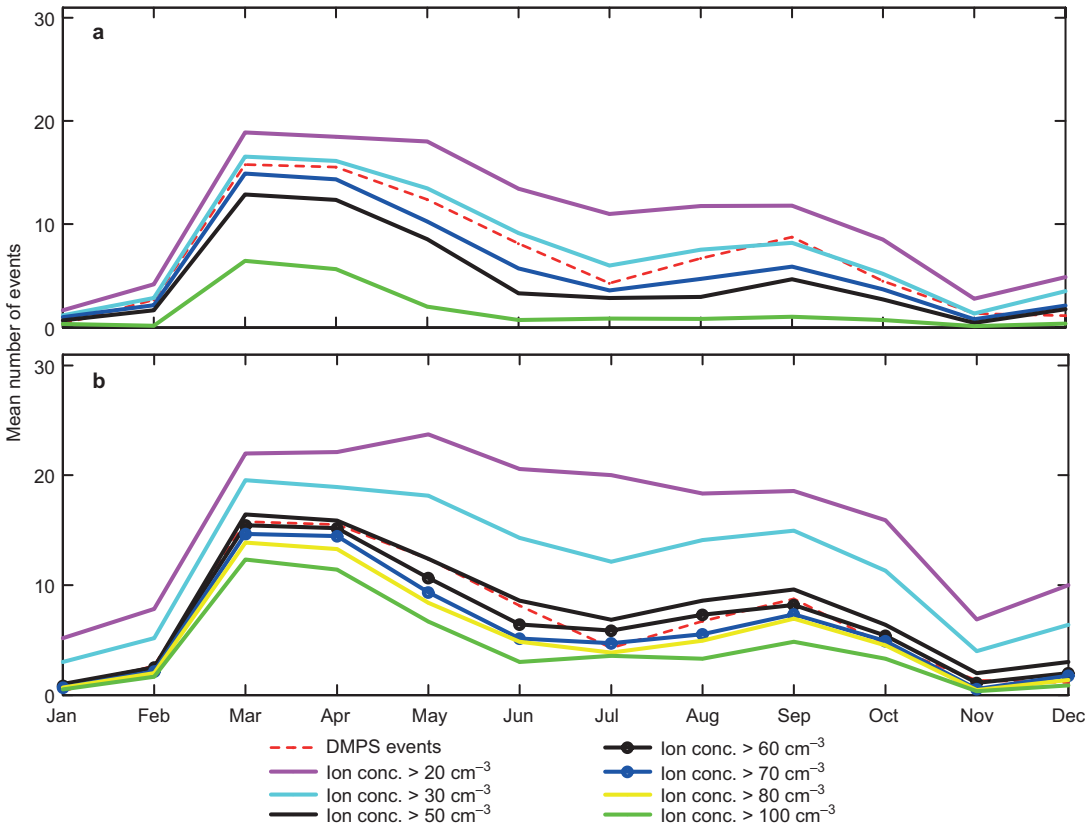

Fig. 6. Seasonal variation in mean number of differently-defined NPF events. Ion events are determined by using limit concentrations of (**a**) 2–4 nm negative ions and (**b**) 2–7 nm negative ions, and particle events are determined with DMPS event analysis.

that in Hyytiälä the increases in the intermediate-ion concentration are rapid as compared with the typical NPF duration of several hours.

We also studied the seasonal variation of the NPF events as classified with the DMPS-based method and using elevated intermediate-ion concentrations for the negative polarity (Fig. 6). More specifically, we searched for the most appropriate ion concentration threshold for identifying the NPF events, and for separating the events from non-events based on the classification made using the DMPS data. In case of the 2–4 nm negative ions, the best agreement between the DMPS-based and intermediate-ion-based event classification was obtained at the maximum ion concentration threshold of 30–40 cm^{-3}. The corresponding threshold for 2–7 nm negative ions was 50–60 cm^{-3}.

We got further support for our results when looking at the relation between the total particle number concentration in the size range of 3–25 nm measured with DMPS and negative ion concentration in the size range of 2–7 nm during NPF event and non-event days at our measurement site (Fig. 7). More specifically, when the ion concentration was higher than a selected threshold concentration, the number of NPF event-day data points exceeded that of the non-event day data points. The fraction of ion concentrations exceeding the limit of 50 cm^{-3} or higher was very low during the non-event days.

Conclusions

Typically, concentrations in the atmosphere of

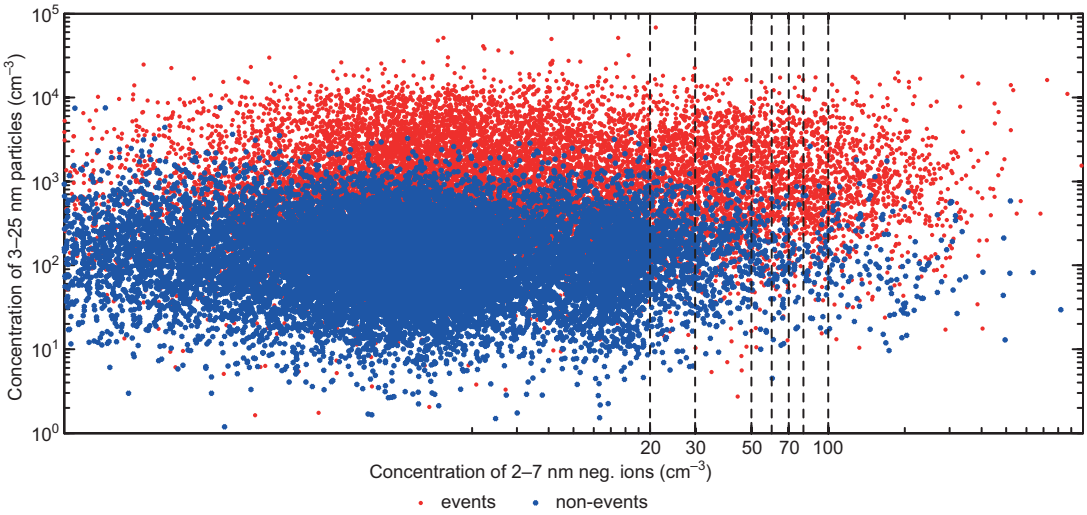

Fig. 7. Total concentrations of the particle in the size range of 3–25 nm measured with DMPS and negative ion concentrations in the size range of 2–7 nm in 2003–2013 at the SMEAR II station in Hyytiälä including only daytime (06:00–18:00) half-hour median concentrations during the NPF event and non-event days.

intermediate ions and neutral particles in the size range of 2–4 nm are very low, with high concentrations observed only during NPF or precipitation events. Therefore, after removing periods with precipitation from the data, we should be able to identify new NPF events based on half-hour median concentration of intermediate ions.

According to our results, intermediate ions can be used as an indicator for atmospheric NPF, and we were able to achieve about 80% accuracy as compared with that of traditional event analysis based on DMPS data. As the traditional analysis is somewhat subjective and the present analysis is not, the new method can be effectively automatized. There are also theoretical reasons why the agreement between the two methods is not expected to reach 100%. First, if a neutral NPF pathway is dominating, the number concentration of intermediate ions may be very small; and second, there were cases when intermediate ions were abundant but the newly-formed particles would not grow into large enough sizes to be characterized as NPF events in the traditional event analysis.

The fact that the seasonal variation of NPF observed at the SMEAR II station (Dal Maso *et al*. 2005) could also be found when using the new method, supports its usefulness. Besides DMPS (particle number size distribution), and NAIS and BSMA (ion number size distributions) have been used in traditional NPF event analyses (Asmi *et al*. 2009). As compared with those with the positive polarity, higher concentrations of intermediate ions with the negative polarity were detected at SMEAR II (Laakso *et al*. 2007, Hirsikko *et al*. 2007, Hirsikko *et al*. 2011); therefore here we focused on the negative polarity. Since our new method was found to be a good way to detect NPF events, it could also be used at other locations. However, the statistics on intermediate-ion concentration should be analysed first to find out the proper ion concentration threshold for the NPF analysis. The particular benefit is the sensitivity in the 2–4 nm size range, where concentrations are typically very small when NPF is not occurring. Therefore, this new method is complements the traditional DMPS-based event analysis.

Acknowledgements: This research was supported by the European Research Council (ERC) Advanced Grant (ATM-NUCLE, 227463), the European Union's Horizon 2020 research and innovation programme under grant agreement no. 654109 (ACTRIS-2), CRAICC project (Cryosphere-Atmosphere Interaction in a Changing Arctic Climate) and the Academy of Finland Centre of Excellence program (projects no. 1118615 and 272041). The research leading to these results has received funding also from the European Union Seventh Framework Programme (FP7/2007-2013 ACTRIS) under grant agreement no. 262254 and European Union's

Horizon 2020 research and innovation programme under grant agreement no. 654109 (ACTRIS2).

References

Aalto P., Hämeri K., Becker E., Weber R., Salm J., Mäkelä J.M., Hoell C., O'Dowd C.D., Karlsson H., Hansson H.-C., Väkevä M., Koponen I.K., Buzorius G. & Kulmala M. 2001. Physical characterization of aerosol particles during nucleation events. *Tellus* 53B: 344–358.

Asmi E., Sipilä M., Manninen H.E., Vanhanen J., Lehtipalo K., Gagné S., Neitola K., Mirme A., Mirme S., Tamm E., Uin J., Komsaare K., Attoui M. & Kulmala M. 2009. Results on the first air ion spectrometer calibration and intercomparison workshop. *Atmos. Chem. Phys.* 9: 141–154.

Buenrostro Mazon S., Kontkanen J., Manninen H.E., Nieminen T., Kerminen V.-K. & Kulmala M. 2016: A long-term comparison of nighttime cluster events and daytime ion formation in a boreal forest. Boreal Env. Res. 21: 242–261.

Curtius J., Lovejoy E.R. & Froyd K.D. 2006. Atmospheric ion-induced aerosol nucleation. *Space Sci. Rev.* 125: 159–167.

D'Alessandro F. 2009. Experimental study of the effect of wind on positive and negative corona from a sharp point in a thunderstorm. *J. Electrostatics* 67, 482–487.

Dal Maso M., Kulmala M., Riipinen I., Wagner R., Hussein T., Aalto P.P. & Lehtinen K.E.J. 2005. Formation and growth of fresh atmospheric aerosols: eight years of aerosol size distribution data from SMEAR II, Hyytiälä, Finland. *Boreal Env. Res.* 10: 323–336.

Flagan R.C. 1998. History of electrical aerosol measurements. *Aerosol Sci. Tech.* 28: 301–380.

Gagné S., Nieminen T., Kurtén T., Manninen H.E., Petäjä T., Laakso L., Kerminen V.-M., Boy M. & Kulmala M. 2010. Factors influencing the contribution of ion-induced nucleation in a boreal forest, Finland. *Atmos. Chem. Phys.* 10: 3743–3757.

Gagné S. Lehtipalo K., Manninen H.E., Nieminen T., Schobesberger S., Franchin A., Yli-Juuti T., Boulon J., Sonntag A., Mirme S., Mirme A., Hõrrak U., Petäjä T., Asmi E. & Kulmala M. 2011. Intercomparison of air ion spectrometers: an evaluation of results in varying conditions. *Atmos. Meas. Tech.* 4: 805–822.

Gopalakrishnan V., Pawar S.D., Siingh D. & Kamra A.K. 2005. Intermediate ion formation in the ship's exhaust. *Geophys. Res. Lett.* 32: 1–4.

Hari P. & Kulmala M. 2005. Station for Measuring Ecosystem–Atmosphere Relations (SMEAR II). *Boreal Env. Res.* 10: 315–322.

Hirsikko A., Laakso L., Hõrrak U., Aalto P.P., Kerminen V.-M. & Kulmala M. 2005. Annual and size dependent variation of growth rates and ion concentrations in boreal forest. *Boreal Env. Res.* 10: 357–369.

Hirsikko A., Bergman T., Laakso L., Dal Maso M., Riipinen I., Hõrrak U. & Kulmala M. 2007. Identification and classification of the formation of intermediate ions measured in boreal forest. *Atmos. Chem. Phys.* 7: 201–210.

Hirsikko A., Nieminen T., Gagné S., Lehtipalo K., Manninen H.E., Ehn M., Hõrrak U., Kerminen V.-M, Laakso L., McMurry P.H., Mirme A., Mirme S., Petäjä T., Tammet H., Vakkari V., Vana M. & Kulmala M. 2011. Atmospheric ions and nucleation: a review of observations. *Atmos. Chem. Phys.* 11: 767–798.

Hoppel W.A. 1967. Theory of the electrode effect. *J. Atmos. Terr. Phys.* 29: 709.

Hõrrak U., Salm J. & Tammet H. 2000. Statistical characterization of air ion mobility spectra at Tahkuse Observatory: Classification of air ions. *J. Geophys. Res.* 105: 9291–9302.

Iida K., Stolzenburg M., McMurry P., Dunn M.J., Smith J.N., Eisele F. & Keady P. 2006. Contribution of ion-induced nucleation to new particle formation: methodology and its application to atmospheric observations in Boulder, Colorado. *J. Geophys. Res.* 111: D23201, doi:10.1029/2006JD007167.

IPCC 2013. *Climate change 2013: the physical science basis*. Contribution of Working Group I to the Fifth Assessment Report of the Intergovernmental Panel on Climate Change, Cambridge University Press, Cambridge, UK, and New York, NY, USA.

Israël H. 1970. *Atmospheric electricity*. Israel Program for Scientific Translations, Jerusalem.

Jayaratne E.R., J-Fatokun F.O. & Morawska L. 2008. Air ion concentrations under overhead high-voltage transmission lines. *Atmos. Environ.* 42: 1846–1856.

Jayaratne E.R., Ling X. & Moraska L. 2010. Ions in motor vehicle exhaust and their dispersion near busy roads. *Atmos. Environ.* 44: 3644–3650.

Jiang J.K., Chen M.D., Kuang C.A., Attoui M. & McMurry P.H. 2011. Electrical mobility spectrometer using a diethylene glycol condensation particle counter for measurement of aerosol size distributions down to 1 nm. *Aerosol Sci. Tech.* 45: 510–521.

Junninen H., Hulkkonen M., Riipinen I., Nieminen T., Hirsikko A., Suni, T., Boy, M., Lee, S.-H., Vana, M., Tammet, H., Kerminen, V.-M. & Kulmala M. 2008. Observations on nocturnal growth of atmospheric clusters. *Tellus* 60B: 365–371.

Kolarž P., Gaisberger M., Madl P., Hofmann W., Ritter M. & Hartl A. 2012. Characterization of ions at Alpine waterfalls. *Atmos. Chem. Phys.* 12: 3687–3697.

Komppula M., Vana M., Kerminen V.-M., Lihavainen H., Viisanen Y., Hõrrak U., Komsaare K., Tamm E., Hirsikko A., Laakso L. & Kulmala M. 2007. Size distributions of atmospheric ions in the Baltic Sea region. *Boreal Env. Res.* 12: 323–336.

Kuang C., Chen M., Zhao J., Smith J., McMurry P.H. & Wang J. 2012. Size and time-resolved growth rate measurements of 1 to 5 nm freshly formed atmospheric nuclei. *Atmos. Chem. Phys.* 12: 3573–3589.

Kulmala M., Hämeri K., Aalto P.P., Mäkelä J.M., Pirjola L., Nilsson E.D., Buzorius G., Rannik U., Dal Maso M., Seidl W., Hoffman T., Janson R., Hansson H.-C., Viisanen Y., Laaksonen A. & O'Dowd, C.D. 2001. Overview of the international project on biogenic aerosol formation in the boreal forest (BIOFOR). *Tellus* 53B:

324–343.

Kulmala M, Vehkamäki H., Petäjä T., Dal Maso M., Lauri A., Kerminen V.-M., Birmili W. & McMurry P.H. 2004. Formation and growth rates of ultrafine atmospheric particles: a review of observations. *J. Aerosol Sci*. 35: 143–176.

Kulmala M., Riipinen I., Sipilä M., Manninen H.E., Petäjä T., Junninen H., Dal Maso M., Mordas G., Mirme A., Vana M., Hirsikko A., Laakso L., Harrison R.M., Hanson I., Leung C., Lehtinen K.E.J. & Kerminen V.-M. 2007. Toward direct measurement of atmospheric nucleation, *Science* 318: 89–92.

Kulmala M., Kontkanen J., Junninen H., Lehtipalo K., Manninen H.E., Nieminen T., Petäjä T., Sipilä M., Schobesberger S., Rantala P., Franchin A., Jokinen T., Järvinen E., Äijälä M., Kangasluoma J., Hakala J., Aalto P.P., Paasonen P., Mikkilä J., Vanhanen J., Aalto J., Hakola H., Makkonen U., Ruuskanen T., Mauldin R.L.III, Duplissy J., Vehkamäki H., Bäck J., Kortelainen A., Riipinen I., Kurtén T., Johnston M.V., Smith J.N., Ehn M., Mentel T.F., Lehtinen K.E.J., Laaksonen A., Kerminen V.-M. & Worsnop D.R. 2013. Direct observations of atmospheric aerosol nucleation. *Science* 339: 943–946.

Laakso L., Petäjä T., Lehtinen K.E.J., Kulmala M., Paatero J., Hõrrak U., Tammet H. & Joutsensaari J. 2004. Ion production rate in a boreal forest based on ion, particle and radiaion measurements. *Atmos. Chem. Phys*. 4: 1933–1943.

Laakso L., Gagné S., Petäjä T., Hirsikko A., Aalto P., Kulmala M. & Kerminen V.-M. 2007. Detecting charging state of ultra-fine particles: instrumental development and ambient measurements. *Atmos. Chem. Phys*. 7: 1333–1345.

Manninen H.E., Petäjä T., Asmi E., Riipinen I., Nieminen T., Mikkilä J., Hõrrak U., Mirme A., Mirme S., Laakso L., Kerminen V.-M. & Kulmala M. 2009. Long-term field measurements of charged and neutral clusters using Neutral cluster and Air Ion Spectrometer (NAIS). *Boreal Env. Res*. 14: 591–605.

Mirme A., Tamm A., Mordas G., Vana M., Uin J., Mirme S., Bernotas T., Laakso L., Hirsikko A. & Kulmala M. 2007. A wide-range multi-channel Air Ion Spectrometer. *Boreal Env. Res*. 12: 247–264.

Mirme S. & Mirme A. 2013. The mathematical principles and design of the NAIS — a spectrometer for the measurement of cluster ion and nanometer aerosol size distributions. *Atmos. Meas. Tech*. 6: 1061–1071.

Myhre G. 2009. Consistency between satellite-derived and modeled estimates of the direct aerosol effect. *Science* 325: 187–190.

Mäkelä J.M., Riihelä M., Ukkonen A., Jokinen V. & Keskinen J. 1996. Comparison of mobility equivalent diameter with Kelvin-Thomson diameter using ion mobility data. *J. Chem. Phys*. 105: 1562–1571.

Mäkelä J.M., Aalto P., Jokinen V., Pohja T., Nissinen A., Palmroth S., Markkanen T., Seitsonen K., Lihavainen H. & Kulmala M. 1997. Observations of ultrafine aerosol particle formation and growth in boreal forest. *Geophys. Res. Lett*. 24: 1219–1222.

Mäkelä J.M., Dal Maso M., Pirjola L., Keronen P., Laakso L. & Kulmala M. 2000. Characteristics of the atmospheric particle formation events observed at a boreal forest site in southern Finland. *Boreal Env. Res*. 5: 4. 299–313.

Nieminen T., Asmi A., Dal Maso M., Aalto P.P., Keronen P., Petäjä T., Kulmala M. & Kerminen V.-M. 2014. Trends in atmospheric new-particle formation: 16 years of observations in a boreal-forest environment. *Boreal Env. Res*. 19 (suppl. B): 191–214.

Tammet H. 2006. Continuous scanning of the mobility and size distribution of charged clusters and nanometer particles in atmospheric air and the Balanced Scanning Mobility Analyzer BSMA. *Atmos. Res*. 82: 523–535.

Tammet H., Hõrrak, Y. & Kulmala M. 2009. Negatively charged nanoparticles produced by splashing of water. *Atmos. Chem. Phys*. 9: 357–367.

Tammet H., Komsaare K. & Hõrrak U. 2014. Intermediate ions in the atmosphere. *Atmos. Res*. 135–136: 263–273.

Vana M., Virkkula A., Hirsikko A., Aalto P., Kulmala M. & Hillamo R. 2007. Air ion measurements during a cruise from Europe to Antarctica. In: O'Dowd C.D. & Warner P. (eds.), *Proceedings of the Nucleation and Atmospheric Aerosols 17th International Conference Galway, Ireland 2007*, Springer, pp. 368–372.

Virkkula A., Hirsikko A., Vana M., Aalto P.P., Hillamo R. & Kulmala M. 2007. Charged particle size distributions and analysis of particle formation events at the Finnist Antarctic research station Aboa. *Boreal Env. Res*. 12: 397–408.

Wagner R., Manninen H.E., Franchin A., Lehtipalo K., Mirme S., Steiner G., Petäjä T. & Kulmala M. 2016: On the accuracy of ion measurements using a Neutral cluster and Air Ion Spectrometer. *Boreal Env. Res*. 21: 230–241.

Wiedensohler A. 1988. An approximation of the bipolar charge distribution for particles in the submicron range. *J. Aerosol Sci*. 19: 387–389.

Yu F. & Turco R. 2008. Case studies of particle formation events observed in boreal forests: implications for nucleation mechanisms. *Atmos. Chem. Phys*. 8: 6085–6102.